

Chapter 5

General Conclusions and Suggestions for Further Work

5.1 General Conclusions

My enhanced imaging work on fault zones in southern California from seismic reflection studies leads to the following conclusions.

Fault-plane reflections reveal the listric true-depth geometry of the normal fault at the Black Mountains range front in southern Death Valley. Accounting for strong lateral velocity variations, this is the first true-depth image of a listric normal fault plane in the Basin and Range province. Its geometry supports the concept of low-angle extension in the region and strengthens the association of listric normal faulting with a proposed magma conduit traced to the surface location of a cinder cone.

The dominance of P -wave reflectivity over S -wave reflectivity from crustal fault zones suggests that variations in Lamé parameter λ control fault zone reflections. Reflections due to λ variations radiate isotropically, unlike the backscatter-

ing from impedance contrasts or the forward scattering from velocity contrasts. I therefore suggest that crustal faults may be distinguishable from non-tectonic crustal structures on the basis of this isotropic P -wave scattering. I showed crustal reflectivity images from the Los Angeles Basin of southern California that select for such isotropic reflectivity, preferentially showing crustal fault structure. My depth sections sum together backscattered and forward scattered arrivals from subsurface depth points, effectively filtering out simple impedance or velocity variations.

This new crustal imaging procedure uses seismic network data in a cost-effective manner to depict prominent crustal structures in the region beneath the Sierra Madre and Northridge aftershock sequences. In particular, imaging beneath the 1991 Sierra Madre aftershock zone shows the same lower crustal reflective zone below the San Gabriel Mountains imaged by the 1994 Los Angeles Region Seismic Experiment. This represents, to the best of my knowledge, the first step of high resolution imaging of complex three-dimensional structures with passive seismic data, using processing techniques commonly used for active-source crustal seismics.

In addition, my work leads to the following key points that summarize the overall importance of fault zone imaging from seismic reflection studies in the region.

It is possible to image active fault zones, but I achieve geometric imaging only, without elastic property constraints. This is due to the imaging method I use, which ignores the amplitude correction factors due to the angle of incidence on

the scatterers, and to the length of the travel path. (Also, scatterers are represented by the sum of reflection wavelets crosscorrelated with a boxcar function to roughly approximate the source wavelet.) Property constraints may only be obtained through the use of an amplitude-preserving or “true-amplitude” imaging method. Only then may migrated wavefield amplitudes provide a measure of true reflectivity and angle-dependent reflection coefficients.

Enhanced imaging of fault zones from seismic reflection studies allows us to comprehend the role fault structures play in extension and/or plate disruption. These issues can only be addressed and answered by the use of seismic imaging. Thus, I constrained tectonic style in two provinces: extensional (Death Valley) and contractional (Los Angeles basin). Each case required 3-D treatment of sources and receivers, asymptotic assumptions (see Appendices B and C), and some knowledge of velocities.

Normal faulting in Death Valley appears as an “intra-plate” feature because imaging does not provide evidence faulting that cuts the Moho, whereas the Elysian Park Thrust may be interpreted as an “inter-plate” feature because it appears to cut the Moho. These are two examples of important geologic questions that can be answered by seismic imaging methods.

According to the recent work of Richards-Dinger and Shearer (1997), thicker than average crust (up to 33 km) appears to be present beneath the eastern Transverse Ranges. This appears to support my interpretation of the prominent north-dipping thrust of my Northridge image, and reinforces the interpretation of thick-

skinned deformation in the region (C. Nicholson, personal communication). This interpretation further suggests that the present crustal shortening in the region (~ 7 mm/yr, according to Donnellan et al., 1993) involves both the lower and upper crust.

Despite simplifying assumptions and the fact that wide-angle reflection and refraction studies generally use lower frequencies (5-10 Hz; Mooney and Meissner, 1992), and thus have correspondingly lower resolution than active-source seismic reflection data, my wide-angle prestack migration results allowed me to confirm the existence of the “lower crustal reflective zone” (brittle-ductile boundary?) below the San Gabriel Mountains.

5.2 Some suggestions for further work

5.2.1 Enhanced imaging of a normal fault with seismic reflection data

My analysis demonstrates a two-step methodology (tomography and prestack depth imaging) for true depth processing of fault reflections to define fault plane geometry and depth in a complex land data set. Depth imaging of structures in the southern Death Valley basin from COCORP Line 9 shows a west-dipping basin-bounding listric normal fault (Black Mountains range-front fault) and a well-defined half-graben basin bottom (Death Valley).

The true-depth imaging of the Black Mountains range-front fault suggests further work to define the complex structural geometries that exist at the southern

end of the central Death Valley graben. The largely extensional Black Mountains range-front fault system transitions to the dextral strike-slip southern Death Valley fault zone near my true-depth image (Fig. 2.1). Although it is clear in Fig. 2.6 that the fault dips west and is listric, Fig. 2.1 shows that my east-west section exhibits somewhat of an apparent dip for this north-northwest fault, and may be showing many subsidiary faults quite obliquely. de Voogd et al. (1986) proposed in addition that the imaged fault (the Wingate Wash fault in their interpretation) may dip down to the north to meet a mid-crustal reflection bright spot beneath Death Valley (Fig. 2.1). To unravel this complex geometry of intersecting fault planes one may develop laterally variable three-dimensional velocity models using first arrival picks from both COCORP Lines 9 and 11 combined with local earthquake data and the optimization techniques of Pullammanappallil and Louie (1994b) and Asad et al. (1997). With the 3-D velocity information one could then perform a full 3-D prestack migration of the Line 9 and 11 reflection data, similar to the way Louie et al. (1997) imaged shallow reflection data. The resulting 3-D image should illuminate the relations between the Black Mountains range-front normal fault, the southern Death Valley strike-slip zone, any north-dipping normal faults, and the Death Valley bright spot.

5.2.2 Enhanced imaging of crustal faults with earthquake data

Despite the irregular distribution of the SCSN stations, my new crustal imaging procedure uses the SCSN data in a cost-effective manner. The depth sections of

Chapter 4 demonstrate the feasibility of obtaining interpretable structural images from wide-angle processing of aftershock data. I expect that the addition of LARSE Line 2 records and optimized 3-D velocities (Zhao and Kanamori, 1995; Magistrale et al., 1996; Hauksson and Haase, 1997) will improve structural definition and detail in the Northridge epicentral area. In addition, I may improve my Sierra Madre images (Fig. 4.4) by using a more reliable velocity model (e.g., Hauksson et al., 1996), and by combining 3-D, wide-angle, prestack imaging of newly-released LARSE Line 1 explosion records, together with Sierra Madre aftershock traces, through an optimized 3-D velocity model. I could then extend my analysis to the LARSE Line 1 explosion and offshore-onshore records, and the Whittier Narrows aftershock records to the south across the Elysian Park fault system in the 1987 event area (Hauksson, 1990). Of course, better, more reliable images could also be obtained after relocating all aftershocks with optimized 3-D velocities, but this is a very demanding task. The only practical thing to do is to use and rely on someone else's relocations (e.g., Hauksson and Haase, 1997).

Even in successful stories, important caveats continually pop up. Some of the work suggested above requires a more powerful prestack imaging tool to handle 3-D lateral velocity variations and avoid some of the most distracting artifacts of my current images. Here are some suggestions for improving the imaging tool, and avoiding and learning more about some of its most distracting artifacts.

Virtual sources

The contribution of a single seismogram can be regarded to consist of two superimposed traces when the source is buried. In the Kirchhoff context, for a surface receiver and a source located in the subsurface, two sets of Kirchhoff ellipses or trajectories are produced; one for the real and the other for the virtual source location. Fig. 5.1 depicts this case.

In the limit, as the subsurface source approaches the free surface, the two sets of Kirchhoff ellipses coalesce into one. This case is equivalent to the migration of vertical seismic profile (VSP) data with real and virtual receivers (Hu and McMechan, 1986). This is not done in the present form of the prestack depth migration described in Chapter 3, but should be incorporated to properly migrate free surface multiples into the depth sections. [The fault zone examples of Chapter 3 (Fig. 3.16a, c, black ellipses) depict one example of a similar type of multiple path.] This is feasible through simultaneous imaging in the real and virtual media as described by Hu and McMechan (1986) for migration of VSP data.

Use of S -waves

I mentioned in Chapter 4 that earthquake seismologists may still be reluctant to believe that one can image faults successfully using only $P-P$, isotropic scattering characteristics, as I have done so far. The dominance of S -waves in the coda of seismograms raises concern about the validity of dealing with $P-P$ scattering in imaging deep crustal reflectors.

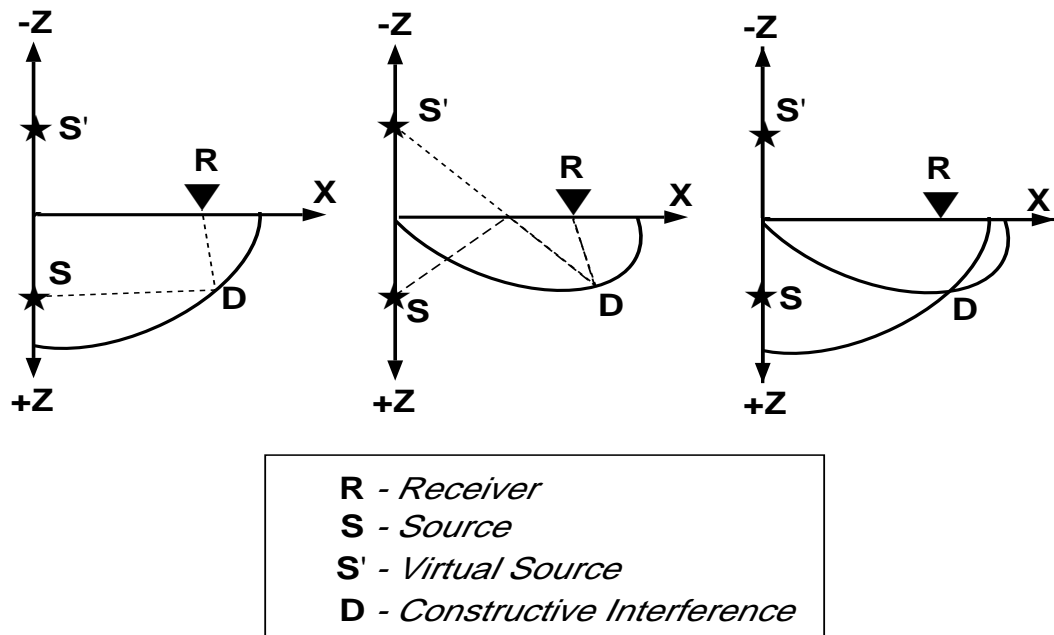


Figure 5.1: Virtual source for the case of a buried source and a surface receiver. An earthquake contributes two arrivals to the trace at the receiver R. The left sketch shows the primary reflection path (dashed line) and the corresponding Kirchhoff trajectory (solid line). The middle sketch shows the free surface multiple path from S to R (long, dashed line), the equivalent path from the virtual source S' to R (short, dashed line), and the corresponding Kirchhoff trajectory (solid line). The right sketch shows the superposition of the two Kirchhoff trajectories with constructive interference at D. (Modified after Hu and McMechan, 1986.)

As shown in Chapter 3, one can also try prestack depth migration of earthquake records with S -waves. To illustrate this idea, Fig 5.2 shows the depth migration of records from the same 18 events I used to obtain the image shown in Fig. 4.4A, including the Sierra Madre main shock, using the southern California velocity model of Fig. 3.1. For this case, S -wave velocities are simply obtained by assuming a Poisson's ratio of $1/3$, so that the ratio of shear versus compressional velocities, V_S/V_P , is equal to 0.5 . The record sections I use also comprise up to 200 km epicentral distance as in the P -wave case, but I now increase duration to 60 s to include (slower velocity) first shear (S_g) arrivals, wide-angle shear reflections and surface and converted waves. I mute all arrivals before the S_g traveltime branch to extract only S , $P - S$, and surface wave arrivals.

Fig. 5.2 does not suggest the lower crustal reflective zone of Fuis et al. (1996). This was expected because there are no isotropic scatterers for the S -wave case (Wu, 1989). In spite of this, very promising work can be done with S -waves. The pioneer work of Spudich and Iida (1993) described basin response and site effects through scattering in alluvial basins using aftershocks of the 1986 North Palm Springs, California, earthquake. They were able to find loci of strong scattering and thus identify crustal heterogeneities that scatter energy into the early part of the observed S -wave codas.

My crustal imaging work was aimed at structural imaging, but it could, in principle, be modified to study anisotropic reflectivity, through careful focal mechanism corrections and tuning the search for scattering structures in alluvial basins.

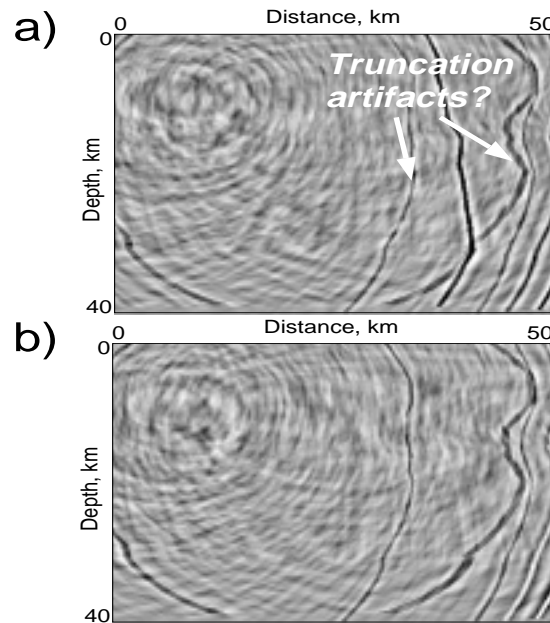


Figure 5.2: a) Depth section 50 km wide and 40 km deep from Azusa north to the margin of the Mojave desert (Fig. 4.1, line A), from *S*-wave migration of the Sierra Madre mainshock and 17 A-quality aftershocks lying between 8.3-14.1 km of the surface. The image does not suggest the lower crustal reflective zone of Fuis et al. (1996). b) Depth section based on a simplified resampling analysis. This image depicts *S*-wave migration artifacts and is equivalent to migration of random noise. Compare with (a) to visually separate out artifacts from signal (coherent reflectors). Apparent data truncation and clipping artifacts of strong amplitude, resembling filtered sign-bit waveforms, appear in the northern side of the sections. These are probably due to saturated, high amplitude late arrivals (surface waves?).

This would imply the search for variations in Lamé parameter μ (rigidity). If successful, this would provide valuable results for potential ground motion modeling trials, which are clearly needed for site characterization and earthquake hazard assessment.

Use of unsigned data

In my crustal imaging work I use signed, high-frequency seismograms from local and regional events. The ability to retain data signs is mandatory for my imaging purposes. The use of unsigned data (e.g., absolute values) only allows me to depict regions of dense ray coverage, or reflection depth-point coverage. Of course, if interested, one can always display the absolute values of the depth images. In this case, “constructive reinforcement” and image enhancement can be obtained at the expense of resolution and of “sign of the reflectivity.” This should prove useful when images of possibly opposing signs are summed (Balch et al., 1991).

My work is complementary to the work of Revenaugh (1995a, b), who has used unsigned, long-period data from similar sets of stations, and teleseisms, with a similar Kirchhoff migration method to find map-scale images of scattering property variations. In addition, Revenaugh (1995c) was able to correlate regions high in scattering potential with slip concentrations on known faults during earthquakes. While Revenaugh’s (1995c) objective was to estimate a characteristic parameter on the surface of a known fault, mine is to detail the location and geometry of known

and unknown faults, without providing much information on characteristic properties. He interpreted variations in regional scattering potential on a crustal scale (8-10 km), whereas I locate major structures with about 1-3 km resolution. Revenaugh (1995c) proposed likely areas of strong, frequent aftershocks, and delineated strength variations along fault systems.

Moreover, Revenaugh and Reasoner's (1997) scattered-wave imaging of upper crustal heterogeneity along nearly 500 km of the San Andreas fault in central California was used to estimate cumulative offset of basement rocks in the fault zone. They found that scattering along the San Andreas fault in central California correlates with segment boundaries established on the basis of historic and paleo seismicity, corroborating evidence from southern California that the upper crustal structures responsible for scattering are important in seismogenesis.

It could be worthwhile, however, to try an implementation of Kirchhoff prestack migration of unsigned, short-period earthquake data in a similar manner to that of Revenaugh (1995a, b). One way would be to compute the migration of absolute-value data and then compute the migrations of many jackknife (derived from a part of the data used to obtain a previous image) or bootstrap realizations of data-scrambling (Efron and Gong, 1983; Tichelaar and Ruff, 1989; Efron and Tibshirani, 1991).

Resampling methods (like the bootstrap, the jackknife, etc) have revolutionized the practice of statistics in the past twenty years or so. They are based on the notion that we can repeat an experiment by constructing multiple data sets from

the one measured data set (Tichelaar and Ruff, 1989). Thus, the original data set is resampled to form a large number of data sets. This is how Revenaugh (1995a, b) resamples his data sets to obtain noise estimates for his Kirchhoff coda migration (KCM). KCM operates on running sums of unsigned data and employs second-root (nonlinear) stacking. Because of this, the migration result is always positive.

KCM requires an estimate of the expected background level (i.e., the expected scattering potential of signal less data) since one cannot assume that large migration values imply strong scattering potential. Revenaugh (1995a) estimates background potential by applying his KCM method to hundreds of trace sets with randomized station associations. His bootstrap-like approach has the effect of destroying any spatial coherence the data might contain. Hence, repeated KCM imaging (about 1000 bootstrap iterations are performed at each migration point; Revenaugh, 1995b) of randomized data sets approximates the probability density function for scattering potential (i.e., a significance scale that defines the relative, point-by-point efficiency of scattering) which is used to assess the significance of data potential.

Artifacts

One final thing to be quite aware of is the unavoidable presence of artifacts with Kirchhoff and other prestack migration approaches. One of the major problems in Kirchhoff depth migration is image resolution. When we apply this method to

data with limited observation geometry, artifacts or false images appear and make the results quite difficult to interpret. This is the case with all the work I presented in this dissertation.

It is quite common in exploration seismology to remove elliptical artifacts through high-pass and dip filters which remove the low-wavenumber information, and reduce high-dipping aperture events (e.g., Hu et al., 1988; Mittet et al., 1997). In fact, artifacts and imaging problems are everyday's bread in the oil industry and Kirchhoff migration is still a subject of current debates. For instance, Norman S. Neidell challenged, during a workshop of the 1996 Annual Meeting of the Society of Exploration Geophysicists, current thinking about 3-D data acquisition and migration (Neidell, 1994, 1997).

Spatial sampling, aliasing and "acquisition footprint" (imaging artifacts due to the source-receiver configuration utilized during data acquisition) are leading edge subjects in exploration seismology. Opinions diverge in part because recent experiments, using synthetic seismic data, have shown that it is possible to recover high frequency information from seismic records when receivers are spaced far enough apart, and the time sample interval is coarse, so that a significant portion of the energy in the signal is spatially and temporally aliased. Thus, it is rather difficult to define, in conclusive terms, what sufficient sampling of seismic data is.

My crustal imaging work suffers from inherent sampling and aliasing problems. The distracting artifacts in my images are inevitable. 3-D prestack migration produces noisy images, even with very simple models. This is not unexpected

and can be explained. The main problem stems from using buried sources, and from limitations with the data and the simplified velocity model (which makes the computations feasible on a basic workstation). As mentioned before, data sampling is poor, irregular and sparse for the crustal imaging work because of the station distribution of the SCSN. Here is where further research will be surely focused for many years to come.